Vivaldi antenna for railway cutting monitoring

Xiaohe Zhou*, J. Le Kernec†,   D. Gray‡

*‡ EEE Department,   Xi'an Jiaotong Liverpool University,   Suzhou,   China,   derek.gray@xjtlu.edu.cn
† EEE Department,   University of Glasgow,   Glasgow,   Scotland,   julien.lekernec@glasgow.ac.uk

Abstract: A planar Vivaldi antenna was reconstructed and assessed as a candidate for a short range,   high range resolution railway cutting monitoring radar.   The initial flare section of the Vivaldi antenna was found to control the return loss of this type of antenna at lower frequencies,   and a compact antenna for 120% fractional bandwidth was demonstrated experimentally.   Group delay was used as a UWB antenna assessment method,   and the prototype antenna gave reasonable performance across the lower half of the band considered.

Keywords: UWB radar;   UWB antennas

I.   INTRODUCTION

Although infrequent,   railway cutting collapses and landslides cause disruption to both passenger and cargo transport,   as well as endangering trains and crew.   Historically,   cutting collapses were a result of use of inappropriate materials,   poor foundations,   insufficient compaction and overly steep gradients.   With climate change,   extreme weather is expected to worsen,   so earthworks are expected to dry and crack during heat waves,   then saturate and potentially liquefy during heavy rainfall.   Small movements and deformation of a slope often occur a reasonable period of time prior to a catastrophic collapse;   detection of that deformation would enable mitigation action.   Prior to the 1950s,   cuttings were fastidiously cleared of vegetation to minimize the risk of fires caused by cinders from steam engines.   Since the change to electric trains,   the growth of shrubs and grass has been unchecked.   Clearing vegetation off short sections of cuttings and performing laser based surveys to monitor possible movement is possible,   but is considered impractical for the full lengths of all cuttings throughout a rail network due to high labor costs.   One potential means of slope monitoring is high range resolution P/L-band vegetation penetrating radar to be carried by service trains which already make periodic passes of all lines within rail networks to monitor track health.
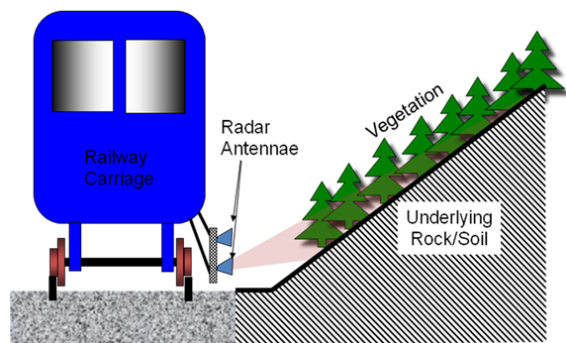

Fig. 1.   End view of radar system measuring cutting surface as the service train carriage passes.[1]

As the object of the proposed system is to accurately measure the position of railway cuttings which are covered in grass and shrubbery,   radio frequencies that penetrate such foliage must be used;   this precludes the use of high frequencies such as X-band [2].   P and L-bands are typically used for foliage penetrating radar,   being frequencies from 500MHz to 2GHz.   Also,   as ground backscatter is sort,   backscatter from the woody parts of the ground cover can be minimized by use of horizontal linearly polarized transmit and horizontal linearly polarized receive (H-H).
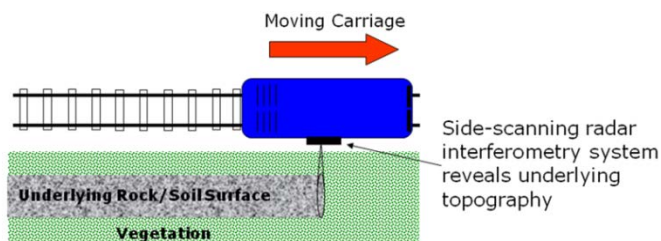

Fig. 2.   Top view of radar system measuring cutting surface as the service train carriage passes.[1]

TABLE I.   RADAR AND ANTENNA REQUIREMENTS

Quantity	Value
frequency range	500MHz – 2GHz
fractional bandwidth	120%
range resolution	10cm
polarisation	H-H
gain	10dBi
physical requirements	robust – all weather exposed mounted on exterior of heavy vehicle

The 500 MHz to 2 GHz band was evaluated by the United States Army Engineers for monitoring railway embankments for deformation and degradation which may lead to railway track movement or damage [3].   That application involves monitoring the different layers of earth below the railway track, and is thus a ground penetrating radar.   Here,   the concern is with movement of the surface cutting to the side of the railway track over long periods of time.

To achieve a range resolution of 10 cm,   a fractional bandwidth of 120% is required,   becoming the main requirement for the P/L-band vegetation penetrating radar, Table 1.   Such a wide bandwidth is comparable to the 110% of the 3.1 to 10.6 GHz ultra-wideband (UWB) radio band [4], so this work builds on the UWB work done at Cork Institute of Technology (CIT) roughly 10 years ago [5].

As linear polarization is required, the higher gain UWB travelling wave antennas based on flared structures originally developed in the 1940s [6-8] are candidates for this system: TEM horn, Libellule antenna, Valentine antenna, Impulse Radiating antenna (IRA), and Vivaldi antenna [9, 10]. The Vivaldi antenna is readily manufactured by PCB process, and is taken as a baseline antenna design in this work. The Vivaldi UWB antenna from CIT was reconstructed based on surviving drawings and photographs. A UWB Vivaldi antenna design could potentially be scaled 6 times and be manufactured on a block of ultra high molecular weight polyethylene (uhmw PE). The first task for this work was to learn how to control the return loss, and the second task was to assess the antennas.

II. VIVALDI ANTENNA DESIGN

The Vivaldi antenna here was derived from surviving drawings and photographs of the design used at Cork Institute of Technology (CIT) in 2006 [5], Figures 3 and 4. The parts of the antenna were a 50Ω characteristic impedance microstrip line at the port, taper to 100Ω characteristic impedance microstrip line at the transition to slotline, where both the microstrip line and the slotline connect to wideband matching stubs; a fan stub for microstrip and circular stub for the slotline, Figure 3. The boresight – radiating side of the slotline has a continuous fixed width section (30mm length, 0.5mm width here), which then tapers into a flare that is the radiating component of the antenna (having 68.5mm length here). The microstrip board used here was 112mm by 120mm, been 0.762mm thickness Arlon 255c substrate (ε_r = 2.55); identical to the substrate used at CIT. In contrast, the Vivaldi antenna used by [11] was 50mm by 50mm; less than a quarter of the size of the antenna used here, and consequently having lower gain.
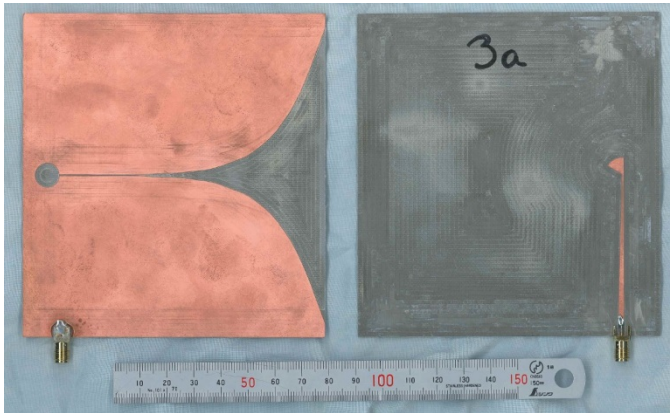

Fig. 3. Photograph of a pair of Design 3 Vivaldi antennas.

The initial Vivaldi antenna, Design 1, gave a high peak S_{11} at 3GHz in CST simulation, Figure 5. Various antenna dimensions were varied, and it was found that the initial taper from slotline to flare is critical to the S_{11} at lower frequencies. Narrowing the start of the taper suppressed the S_{11} peak at 3GHz in 2 subsequent designs, Figures 4 and 5 and Table II.
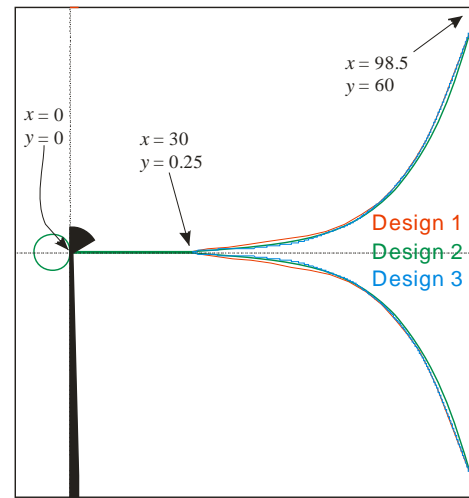

Fig. 4. Variation of slotline flare of different Vivaldi antenna designs; all dimensions in mm.

TABLE II. CONTROL POINTS FOR PARAMETRIC STUDY OF SLOTLINE FLARE TAPERS FOR THE VIVALDI ANTENNAS

X-position (mm)	Y-position (mm)		
	Design 1	Design 2	Design 3
0	0.25	0.25	0.25
30	0.25	0.25	0.25
35	0.8	0.68	0.697
40	1.15	0.9	0.807
45	1.55	1.38	0.972
50	2.25	2	1.611
55	2.85	2.59	2.123
60	4	3.882	3.53
65	5.6	5.42	5.48
70	7.55	7.65	7.293
80	15.359	15.359	15.359
90	30.658	30.658	30.658
98.5	55	55	55

Note: position (30, 0.25) is the beginning of the slotline flare.

Vivaldi antennas Design 2 and Design 3 were manufactured on 0.762mm thickness Arlon 255c substrate using a PCB milling machine. There was a reasonable level of agreement between CST and experiment from 500MHz to 5GHz, Figures 6 and 7. For frequencies above 5GHz, the agreement was not as good, but the measured S_{11} adequately satisfied S_{11}d-10dB. It is noted that [9] had problems with simulated and measured agreement at higher UWB frequencies. Design 3 gave 138% fractional bandwidth across 2 to 11GHz, exceeding the 120% requirement.
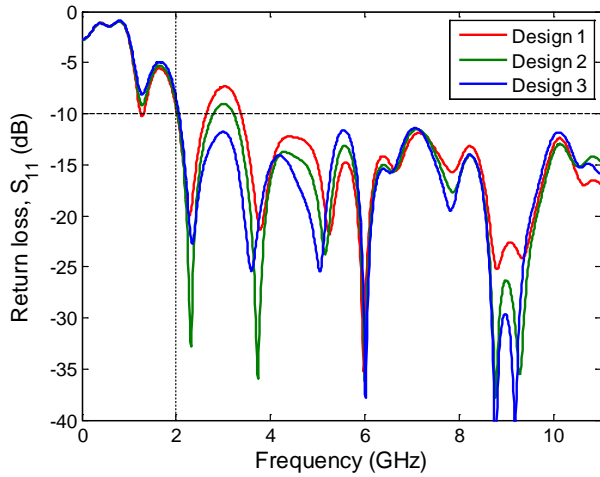
Fig. 5.   Return loss of Vivaldi antennas from flare variation parametric study, from CST™.
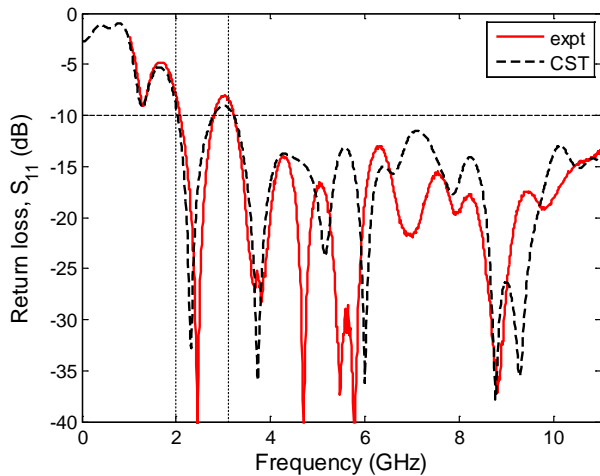

Fig. 6.   Measured and simulated return loss of Design 2 Vivaldi antenna.
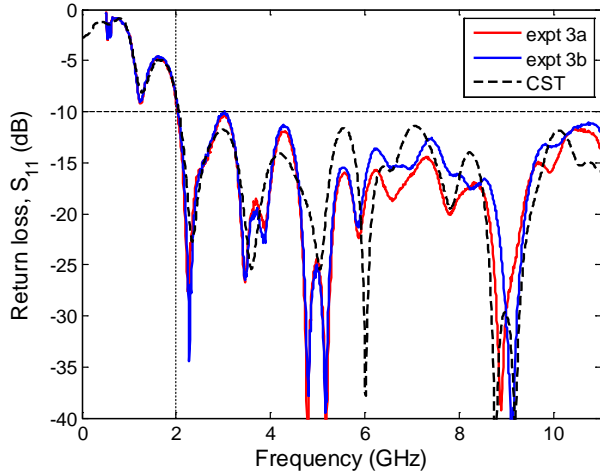

Fig. 7.   Measured and simulated return loss of Design 3 Vivaldi antennas.

The theoretical boundaries of the reactive near field – near field – far field are discussed in most antenna textbooks,   and give an indication as to what distance an antenna should be kept

from any objects that may modify its current distribution and at what distance a consistent radiation pattern shape can be measured [12].   Having settled on the Design 3 Vivaldi antenna,   its maximum dimension of 120mm was used to calculate the theoretical reactive near field – near field – far field boundaries across 500MHz to 12GHz,   Figure 8.   The near field – far field boundary distance increased linearly with frequency,   while the reactive near field – near field boundary distance increased non-linearly with frequency.   To ensure far field across 120% fractional bandwidth (2 to 8GHz),   2 identical Design 3 Vivaldi antennas would have to be about 1.4m apart,   which is far greater than the antenna separation used for UWB antenna assessment in [11].   To ensure at least near field separation across 2 to 8GHz and to avoid any reactive near field coupling effects,   2 identical Vivaldi antennas would have to be 300mm apart.
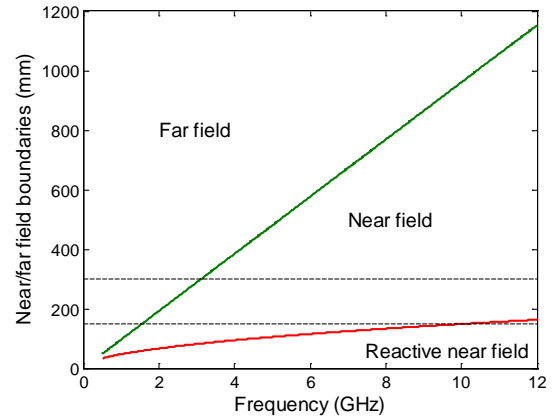

Fig. 8.   Theoretical reactive near field – near field – far field boundaries for a 120mm aperture.

III.   GROUP DELAY STUDY

A number of different means of assessing both low and high gain UWB antennas were assessed in [11].   The group delay was used here.   The group delay is defined as the derivative with respect to frequency of the phase of the S_{21} between 2 identical antennas (equation 3.15 of [11]):

$$\tau = -\frac{d\Phi(\omega)}{d\omega} = -\frac{1}{360°}\frac{d\Phi(f)}{df} \tag{1}$$

Two Design 3 antennas were aligned, and moved apart in steps both experimentally and in CST,   Figure 9.   The CST results are presented here.

Theoretically,   the minimum spacing of 150mm between the antennas used in the CST simulations was in the reactive near field region for the 3.1 to 10.6 GHz range,   Figure 8.   The spacing was increased in 50mm steps to 300mm,   which is in the near field region for the UWB frequency range,   Figure 10.   The group delay results for the different spacings for frequencies greater than 1.5GHz were close to parallel.

The fine ripple in the 200 to 300mm spacing group delay traces above 6GHz were the result of the standing wave between the 2 antennas,   as is commonly seen in anechoic chamber gain measurements.   Means of suppressing this effect will be investigated as future work.
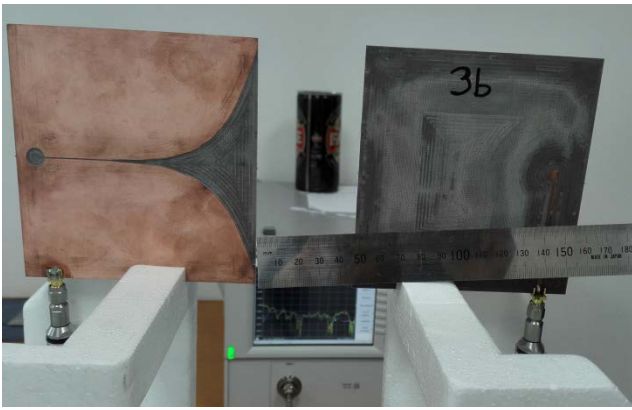
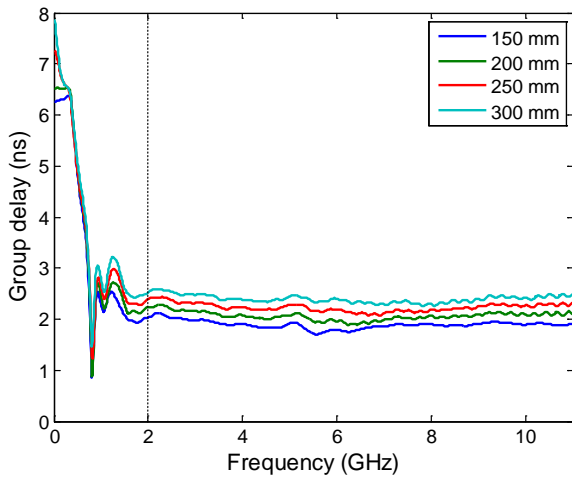Fig. 9. Two Design 3 antennas under test for group delay study.

Fig. 10. Group delay results from two antenna coupling study,   from CST™.
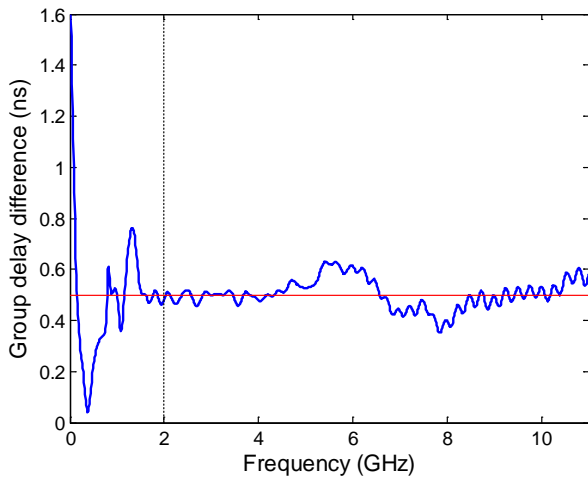

Fig. 11. Difference between 150 and 300mm spacing group delay results from two antenna study,   from CST™.

Theoretically, a 150mm increase in separation would give 0.5ns increase in propagation delay. Comparing the 150mm and 300mm separation group delay results, the difference was close to 0.5ns for frequencies above 1.5GHz. Considering the 2 to 8GHz range, the group delay difference

was very close to 0.5ns for 2 to 5GHz. For 5 to 8GHz the group delay difference ranged from 0.1ns less than the theoretical value to 0.15ns more. The cause of this deviation away from theory will be investigated as part of future work.

This process will be repeated for the experimental data and will be discussed during the presentation.

IV. UWB PULSE SIGNAL ANALYSIS

In [5], the fifth derivative of a Gaussian pulse (FDGP) was used shown to be suitable to fit the IEEE 802.15.3 part 15 indoor emission limits. Even though, this is not an indoor application, the pulse is used to test the time domain response of the pair of antennas.   The excitation signal time response was done in CST simulation.   Figure 12 shows the excitation signal and the reflected signals from one of the antennas as well as the received signal at the second antenna port.
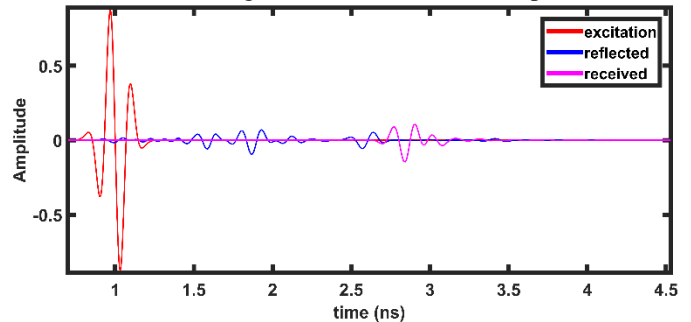

Fig. 12. Time domain response of one of the antennas to an excitation signal (FDGP) from CST™.

The pulse compression is analyzed to gauge the resolution and the contrast and the resolution that could be obtained with this signal.
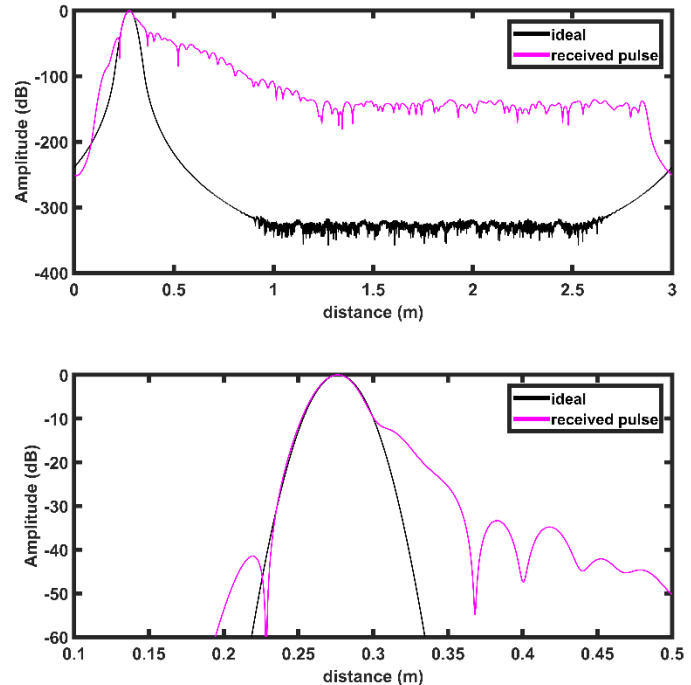

Fig. 13. Autocorrelation of the excitation signal and pulse compression of the received signal with the excitation signal. (top) general view (bottom) expanded view of the main lobe and side lobes

Figure 13. shows the autocorrelation of the excitation signal and the pulse compression of the received signal by the excitation signal. The resolution at 3dB-width is 2.61 cm (compared) and the side lobes are at -41.55 on the left of the main lobe and -12.53 dB on the right. The slope of the pulse compression on the right is consistent with the presence of standing waves in the antenna. Far field simulations on a target will be conducted in future work.

V. CONCLUSIONS

A UWB Vivaldi antenna from about 10 years ago was reconstructed from surviving photographs and drawings. In both CST simulation and experiment, it was found that the shape of the taper from slotline in the ground plane to the flare was critical for controlling the return loss at lower frequencies. A return loss peak at 3GHz was successfully reduced to S_{11}d-10dB allowing the final Vivaldi antenna design to be used down to 2GHz. This antenna could be scaled by 4 for the target frequency band, whereas the original design would have to be scaled by 6, giving the advantage a smaller final antenna.

Group delay was trialed as a wideband antenna assessment technique. The difference between the nearest and furthest separation group delay results from CST simulations of the final Vivaldi antenna design closely matched the theoretical propagation delay for 2 to 5GHz. For the remainder of the required 120% fractional bandwidth (5 to 8GHz), the group delay difference diverged both positively and negatively from the propagation delay. The cause of this effect will be investigated as part of future work.

The time domain analysis using the fifth derivative of a Gaussian pulse covering the target range 3.1-10.6 GHz was used to test the antenna pair. The received pulse is very distorted due to the presence of standing waves. The pulse compression of the received pulse displays a resolution of 2.61 cm and sidelobes at -41.55 dB (left) and -12.53 dB (right) with a trailing slope which is consistent with the presence of standing waves. Further analysis of far field simulations on targets and using different signals will allow to select the most appropriate signal for the application.

REFERENCES

[1] Andrew Sowter et al., "Microrail, Monitoring Vegetated Road and Railway Cuttings using Radar Interferometry", University of Nottingham, Nottingham, UK, Tech. Rep., 2010

[2] F.T. Ulaby, R.K. Moore and A.K. Fung, "Microwave remote sensing," Norwood, MA, Artech House, 1986.

[3] J.R. Lundien, "Feasibility Study for Railroad Embankment Evaluation with Radar Measurements," U.S. Army Engineer Waterways Experiment Station Geotechnical Laboratory, Report WES-MP-S-78-10, Aug. 1978.

[4] FCC 2002

[5] J. Le Kernec, D. Gray, "Impulse Radio UWB radar pulse detector", *IET international radar conference 2015*, Hangzhou, China, 14-16 October 2015

[6] G.C. Southworth, "Short wave radio system," United States patent US2,206,923, granted July 6th, 1940.

[7] A.P. King, "Transmission, radiation and reception of electromagnetic waves," United States patent US2,283,935, granted May 26th, 1942.

[8] L.N. Brillouin, "Broad band antenna," United States patent US2,454,766, granted November 30th, 1948.

[9] B. Cadilhon, B. Cassany, Patrick Modin, J.-C. Diot, V. Bertrand and L. Pécastaing, "Ultra Wideband Antennas for High Pulsed Power Applications," Chapter 15 in *Ultra Wideband Communications: Novel Trends - Antennas and Propagation*, Eds M. Matin, InTech, 2011.

[10] M. Manteghi and Y. Rahmat-Samii, "A novel UWB feeding mechanism for the TEM horn antenna, reflector IRA, and the Vivaldi antenna," *IEEE Antennas and Propagation Magazine*, Vol. 46, Iss. 5, 2004, pp. 81-87.

[11] G. Quintero Diaz de Leon, "Analysis and design of ultra-wideband antennas in the spectral and temporal domains," Ph.D. thesis, Ecole Polytechnique Federale de Lausanne, 2010.

[12] C.A. Balanis, "Antenna theory: analysis and design," 4th edition, Wiley, 2016.